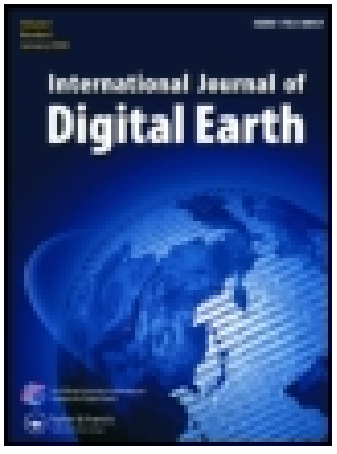

International Journal of Digital Earth
Publication details, including instructions for authors and subscription information:
http://www.tandfonline.com/loi/tjde20

Building segmentation and modeling from airborne LiDAR data

Yong Xiao[a], Cheng Wang[a], Jing Li[a], Wuming Zhang[b], Xiaohuan Xi[a], Changlin Wang[c] & Pinliang Dong[d]

[a] Key Laboratory of Digital Earth Science, Institute of Remote Sensing and Digital Earth, Chinese Academy of Sciences, Beijing, China

[b] State Key Laboratory of Remote Sensing Science, School of Geography, Beijing Normal University, Beijing, China

[c] Institute of Remote Sensing and Digital Earth, Chinese Academy of Sciences, Beijing, China

[d] Department of Geography, University of North Texas, Denton, TX, USA

Published online: 14 May 2014.

To cite this article: Yong Xiao, Cheng Wang, Jing Li, Wuming Zhang, Xiaohuan Xi, Changlin Wang & Pinliang Dong (2014): Building segmentation and modeling from airborne LiDAR data, International Journal of Digital Earth, DOI: 10.1080/17538947.2014.914252

To link to this article: http://dx.doi.org/10.1080/17538947.2014.914252

International Journal of Digital Earth, 2014
http://dx.doi.org/10.1080/17538947.2014.914252

Taylor & Francis
Taylor & Francis Group

Building segmentation and modeling from airborne LiDAR data

Yong Xiao[a], Cheng Wang[a]*, Jing Li[a], Wuming Zhang[b], Xiaohuan Xi[a], Changlin Wang[c] and Pinliang Dong[d]

[a]*Key Laboratory of Digital Earth Science, Institute of Remote Sensing and Digital Earth, Chinese Academy of Sciences, Beijing, China;* [b]*State Key Laboratory of Remote Sensing Science, School of Geography, Beijing Normal University, Beijing, China;* [c]*Institute of Remote Sensing and Digital Earth, Chinese Academy of Sciences, Beijing, China;* [d]*Department of Geography, University of North Texas, Denton, TX, USA*

(*Received 15 July 2013; accepted 8 April 2014*)

Due to the high accuracy and fast acquisition speed offered by airborne Light Detection and Ranging (LiDAR) technology, airborne LiDAR point clouds have been widely used in three-dimensional building model reconstruction. This paper presents a novel approach to segment building roofs from point clouds using a Gaussian mixture model in which buildings are represented by a mixture of Gaussians (MoG). The Expectation-Maximization (EM) algorithm with the minimum description length (MDL) principle is employed to obtain the optimal parameters of the MoG model for separating building roofs. To separate complete planar building roofs, coplanar Gaussian components are merged according to their distances to the corresponding planes. In addition, shape analysis is utilized to remove nonplanar objects caused by trees and irregular artifacts. Building models are obtained by combining segmented planar roofs, topological relationships, and regularized building boundaries. Roof intersection segments and points are derived by the segmentation results, and a raster-based regularization method is employed to obtain geometrically correct and regular building models. Experimental results suggest that the segmentation method is able to separate building roofs with high accuracy while maintaining correct topological relationships among roofs.

Keywords: LiDAR; roof segmentation; mixture of Gaussians; reconstruction; boundary regularization

1. Introduction

As a major component of digital earth, three-dimensional (3D) building models have a wide variety of applications in urban planning, virtual reality, change detection, and emergency planning. Due to the fast acquisition speed and accurate 3D coordinates (i.e. horizontal and vertical information), Light Detection and Ranging (LiDAR) point clouds have been an important data source for high-quality 3D building model reconstruction (Maas and Vosselman 1999; Gamba and Houshmand 2000; Wang 2013). The process of reconstructing building models from airborne LiDAR point clouds mainly consists of several subprocesses: building detection, roof segmentation, and model generation. Building detection aims to extract building points from LiDAR point clouds, and many classification methods in pattern recognition can be used to effectively separate building

*Corresponding author. Email: chengwang@ceode.ac.cn

points from other points. The results of roof segmentation and model generation have a direct impact on the accuracy of the building model. Effectively extracting building roofs and obtaining accurate building models from LiDAR data are still challenging research topics.

The main contribution of this paper is to introduce a novel segmentation method to separate building roofs and propose an extensible building model generation method. The roof segmentation method is able to separate building roofs while maintaining correct topological information. In addition, an extensible method for building model generation is presented by using rasterized point clouds and generic adjustments of building boundary segments. The remaining contents of this paper are organized as follows. Section 2 briefly reviews the related work. In Section 3, detailed principles of our segmentation approach and implementation steps are presented. In Section 4, the model generation method which identifies roof intersection segments and boundary segments is described. The datasets and application details are illustrated in Section 5. Section 6 demonstrates experimental results of the proposed approach as well as a comparison between the proposed method and the RANdom SAmple Consensus (RANSAC) method. The main conclusions and future work are provided in Section 7.

2. Related work

To obtain final 3D polyhedral building models from LiDAR point clouds, key segments and vertices of the roofs should be estimated using the building points. In terms of the roof intersection segments, building roof segmentation methods are employed to divide building roof points into planar clusters. The remaining segments, mainly building boundaries, are estimated by boundary regularization methods which usually extract segments from point clouds and align these segments based on a priori knowledge.

2.1. Roof segmentation

Generally, roof segmentation methods can be categorized into two groups: model-driven methods and clustering methods. The model-driven methods iteratively search for mathematical models (mainly planes) from point clouds. Hough transform and the RANSAC algorithm are two widely used methods in roof segmentation. Vosselman and Dijkman (2001), Oda et al. (2004), and Overby et al. (2004) used 3D Hough transform to detect planes from point clouds. Rabbani and Van Den Heuvel (2005) extended 3D Hough transform to extract other 3D geometric primitives like cylinders. The popular RANSAC algorithm can effectively detect geometric primitives from data containing more than 50% outliers (Fischler and Bolles 1981; Roth and Levine 1993). Ameri and Fritsch (2000) and Brenner (2000) introduced the RANSAC algorithm to detect the roof planes from airborne LiDAR data. Schnabel, Wahl, and Klein (2007) made improvements on the performance of the RANSAC algorithm by utilizing an octree to organize point clouds, thereby improving the probability of selecting points from certain geometric primitives. Tarsha-Kurdi, Landes, and Grussenmeyer (2008) extended RANSAC to make it applicable and efficient in extracting building roofs from LiDAR point clouds. Before performing RANSAC, they performed resampling and used a low-pass filter to improve data quality, and the evaluation function takes into account the standard deviation as well as the number of points. Chen et al. (2012) introduced a localized sampling method based on a grid structure to improve the probability of selecting points on the same geometric shapes. However, RANSAC and Hough transform can only efficiently detect

mathematical planes, and they usually fail to correctly identify neighboring roof points as these points are assigned to planes based on the deviation of the points from the planes.

Clustering methods, such as region growing, fuzzy *K*-means, and mean shift, are also employed to segment building roofs in building modeling from airborne LiDAR data. Alharthy and Bethel (2004) and Verma, Kumar, and Hsu (2006) utilized the region growing algorithm to detect planes in small neighborhoods. Sampath and Shan (2010) presented an approach to reconstruct polyhedral building models with a potential-based fuzzy *K*-means method. Fuzzy *K*-means is used to cluster normal vectors of point clouds into several segments while the number of segments can be estimated by a potential-based approach. By analyzing distance and connectivity of segments, parallel and coplanar segments are separated, and then building vertices are determined by topological analysis of planar segments. Dorninger and Pfeifer (2008) proposed a comprehensive automated 3D building modeling framework from LiDAR point clouds. The mean shift and region growing algorithms were used to segment building roof points into several planar patches. Kim and Shan (2011) presented a novel approach for building roof modeling, including roof plane segmentation and roof model reconstruction from LiDAR data. Segmentation is performed by minimizing an energy function formulated as a multiphase level set and meanwhile roof ridges and step edges are delineated.

In this paper, a novel approach for building roof segmentation is presented. Based on the fact that the distribution of points on a planar patch can be described by the Gaussian distribution, the mixture of Gaussians (MoG) is utilized to model a single building. The MoG model has been used in airborne LiDAR data processing to classify raw point clouds. Charaniya (2004) and Lodha, Fitzpatrick, and Helmbold (2007) both used supervised classification with the Expectation-Maximization (EM) algorithm to classify airborne LiDAR point clouds into roads, grasses, buildings, and trees based on several features, such as aerial image intensity, height, and LiDAR return intensity. In contrast to the previous methods introducing the MoG to LiDAR data classification, in this paper the MoG model is specifically employed to depict the roof points of buildings and the classification aims to extract planar roofs. Furthermore, instead of utilizing the features derived from the data, only 3D coordinates are used, thereby improving accuracy in feature calculation. Additionally, an unsupervised classification is carried out by the EM algorithm combined with the minimum description length (MDL) principle. In comparison with previous building roof segmentation methods, the proposed method utilizes a stochastic model, i.e. the MoG model to represent building roofs.

2.2. Model generation

Due to the nonuniform sampling of the airborne LiDAR system, building boundary points usually display as zigzags in detail. To obtain geometrically regular and correct building boundaries, prior knowledge about building structure is usually utilized to adjust long segments extracted from the boundary points. To maintain the regularity of building models, dominant directions (Alharthy and Bethel 2002; Zhang, Yan, and Chen 2006; Zhou and Neumann 2008) are introduced to align the segments. It is assumed that buildings have two dominant directions which are perpendicular to each other and most of the segments of the buildings are either parallel or perpendicular to the dominant directions. These methods usually fail to model complex buildings with complex shapes or those composed of several simple building models (e.g. gable roof, flat roof). Some other approaches (Sampath and Shan 2004; Sester and Neidhart 2008) utilize least square

estimation of the segments to adjust the segments. However, these methods require long segments to be extracted before performing least square estimation and thus may obtain unconvincing results for small buildings.

In this paper, to make the methods generic and applicable, generative adjustment is adopted on the long segments obtained from rasterized point clouds using the RANSAC method. Instead of using the original point clouds, the raster data are used to facilitate the subsequent processing, mainly in parameter setting. In addition, this paper utilizes the roof topology information to identify the location of the roof intersection points.

3. The MoG segmentation

A novel segmentation method is proposed to extract building roofs from building points collected by airborne LiDAR data. The overall workflow of the segmentation method is presented in Figure 1. The EM classification is performed to estimate the optimal parameters (the number of Gaussian component K and the mean and covariance of every Gaussian) of the MoG model. The best value of K is chosen according to the MDL principle and then the corresponding classification results are refined by removing

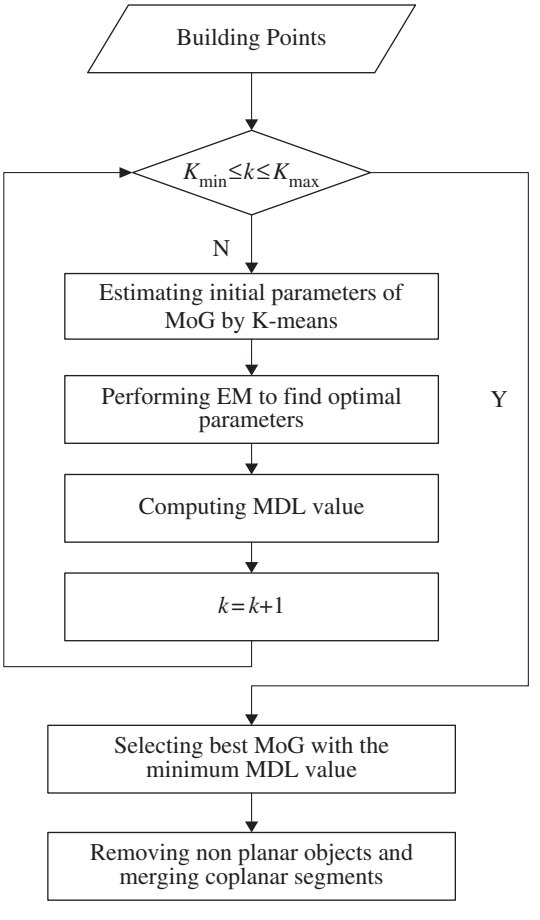

Figure 1. Workflow of the segmentation method.

nonplanar objects and merging coplanar clusters. Finally, complete building roofs are extracted.

In Section 3.1, we demonstrate that, based on the fact that a 3D Gaussian distribution can model points within real planar roofs, the MoG model is able to represent building points. Then parameter estimation of the MoG model by the EM-MDL method and refinements of the EM-MDL results are presented in Sections 3.2 and 3.3, respectively.

3.1. The MoG

The Gaussian distribution can describe a variety of probability distributions and is widely used in natural sciences as a simple model for describing complex phenomena. The Gaussian distribution defined over a d-dimensional vector $\mathbf{x}$ of continuous variables is given by

$$N(\mathbf{x}|\boldsymbol{\mu}, \Sigma) = \frac{1}{(2\pi)^{d/2}} \frac{1}{|\Sigma|^{1/2}} \exp\left\{-\frac{1}{2}(\mathbf{x}-\boldsymbol{\mu})^T \Sigma^{-1}(\mathbf{x}-\boldsymbol{\mu})\right\} \tag{1}$$

where the d-dimensional vector $\boldsymbol{\mu}$ is the mean and the $d \times d$ matrix Σ is the covariance. In this paper, it is assumed that if $\mathbf{x}$ denotes 3D coordinates of a point, the 3D Gaussian model can be used to describe the distribution of points within a planar patch.

Due to the limited elevation accuracy of airborne LiDAR data, collected points of planar roofs do not exactly lie on a mathematical plane. Instead, they scatter within a thin plate while their deviations to the plane conform to a Gaussian distribution centered at zero. In fact, points in real planar roofs do not lie on a strict mathematical plane because the measurements taken in building construction are not exact. In other words, a planar roof surface is not so smooth that it can be represented by a disk and thus a 3D Gaussian model. As we know, a typical 3D Gaussian distribution of points scatters in an ellipsoid whose principal axes are given by the eigenvectors of the covariance matrix Σ (Alpaydin 2004). When these points are nearly located on a plane, the ellipsoid looks more like a thin disk and the eigenvector corresponding to the minimum eigenvalue is parallel to the normal vector of the plane. In short, since points of a planar patch acquired by airborne LiDAR system usually scatter in a thin disk, the 3D Gaussian distribution is able to model these points. Therefore, a single building containing more than one roof is represented by an MoG model.

An MoG model is a linear superposition of Gaussian distribution in the following form:

$$p(\mathbf{x}) = \sum_{k=1}^{K} \pi_k N(\mathbf{x}|\mu_k, \Sigma_k) \tag{2}$$

where $\boldsymbol{x}$ is the observed data vector, K is the number of Gaussian components in the MoG, N ($\boldsymbol{\mu}_k$, Σ_k) denotes the kth component, i.e. the kth Gaussian distribution of the MoG, $\boldsymbol{\mu}$ and x are the mean and covariance of the kth component, respectively, and π_k is the mixture coefficient. The mixture coefficients π_k satisfy $\sum_{k}^{K} \pi_k = 1, 0 \leq \pi_k \leq 1$. Mixture coefficients can be interpreted as ratios of points contained by the corresponding Gaussian components. When representing building roof points, the number of Gaussian components of the MoG model is usually larger than the true number of roofs even

though each 3D Gaussian component is employed to model points within a planar patch. The main reason is that points sampled from a Gaussian model usually locate near the center $\boldsymbol{\mu}$ in the feature space, i.e. in the Euclidean space in our method. As the Gaussian model utilizes the squared Mahalanobis distance $(\boldsymbol{x}-\boldsymbol{\mu})^T\Sigma^{-1}(\boldsymbol{x}-\boldsymbol{\mu})$ to compute the probability of a point belonging to the model, points far from the center possess large values of Mahalanobis distance and thus small possibility to this model. Thus, a long narrow roof is usually represented by two or three Gaussian models instead of one. Therefore, in order to extract complete building roofs, after parameters of the MoG model are estimated, coplanar components are merged according to the distance between the components.

The key of roof segmentation is to assign roof points to their corresponding roofs. When planar roof patches are represented by their corresponding Gaussian models, the neighboring roof points can be separated into different components. The probability of a point belonging to a Gaussian component depends on the squared Mahalanobis distance which takes both the feature of the point and the covariance matrix of the model into consideration. Even though the neighboring roof points are close in the Euclidean space to the two Gaussian components, the probabilities of the points belonging to the two components are different. Since discriminative building roofs usually possess different aspects and thus different covariance matrixes, neighboring roof points can be assigned to different Gaussian components. Based on the fact that neighboring roof points are correctly classified, each component of the MoG model denotes a complete roof or a roof patch. Therefore, by merging coplanar components, complete building roofs are separated.

3.2. Parameter estimation of the MoG model

To obtain the optimal parameters of the MoG model, the general EM algorithm (Dempster, Laird, and Rubin 1977) is often employed to effectively obtain the optimal estimation even though there is no guarantee to achieve the global optimal results. Prior to performing the EM algorithm, the initial values of the parameters of the MoG model should be assigned. The *K*-means algorithm (Lloyd 1982), which converges more quickly, is usually utilized to find the suitable initial values of the EM algorithm (Bishop 2006). However, by performing *K*-means initialization, it is assumed that the number of clusters should be given beforehand. In order to perform unsupervised classification, some extended techniques should be employed to determine K (the number of Gaussian components), for example the MDL principle (Rissanen 1983).

In order to automatically identify the number of Gaussian components, the MDL principle is utilized in our method in the parameter estimation of the MoG model. The MDL principle is a trade-off between the likelihood of the model to the data and the complexity of the model itself (Grünwald 2007). The MDL principle selects the number of components that minimizes the following formula:

$$MDL = -L + \frac{1}{2} m \log N \tag{3}$$

where $m = (K-1) + K\left\{D + \frac{1}{2}D(D+1)\right\}$, L is the log-likelihood of the EM algorithm, K is the number of components of the MoG model, and D is the dimension of the features. The second part, $\frac{1}{2} m \log N$, of Equation (3) is determined by the complexity of

the MoG, i.e. the number of components, K and the data, i.e. the dimension and the number of data.

By changing the number of components K in a user-defined range[$K_{\min}$, $K_{\max}$], various MDL values can be obtained. The optimal number of components corresponding to the minimum MDL value is then determined and chosen to be the number of planar patches extracted by the EM algorithm.

3.3. Refinements of the EM-MDL results

After the EM-MDL classification is performed, further refinements, including removing nonplanar objects and merging coplanar patches, are employed to extract complete building roofs.

Since the EM-MoG methods do not discard any points, nonplanar objects, such as drainage pipelines, chimneys, small irregular objects, and trees, are not removed. In order to identify those nonplanar objects, shape analysis based on their planarity is performed. The planarity is defined as the ratio of the minimum eigenvalue of the covariance matrix Σ to the sum of all eigenvalues of Σ. The Gaussian models corresponding to the irregular artifacts are quite different from planar roofs as points of these objects usually scatter in an ellipsoid instead of a thin disk. For a Gaussian model representing a planar patch, the minimum eigenvalue is nearly zero and its corresponding eigenvector is parallel to the normal vector of the patch. Thus, nonplanar objects can be identified by its planarity. Shape analysis is employed to detect and remove nonplanar objects before merging coplanar patches.

In addition, as illustrated in Section 3.1, one roof may be modeled by more than one Gaussian component. Therefore coplanar clusters should be grouped into one cluster in order to extract complete roofs. Coplanar clusters are identified by their normal vectors and distances. The distance between two point sets is defined as (Sampath and Shan 2010)

$$D_{P,Q} = \min\left(d\left(p_i, q_j\right)\right) \forall p_i \in P; \forall q_j \in Q \tag{4}$$

where P, Q denote cluster P and cluster Q, p_i and q_j are any point belonging to cluster P and cluster Q, respectively, and d (p_i, q_j) is the Euclidean distance between p_i and q_j. When two planar patches present a small distance and their normal vectors are parallel to each other, they will be merged into one planar patch.

In short, once initial classification results are obtained, nonplanar clusters are removed by their planarity and then coplanar clusters are merged. Finally, complete building roofs are extracted.

4. Model generation

3D building models constructed by airborne LiDAR data are polyhedral models whose walls are obtained by extending the building boundaries to the ground. Therefore, to obtain 3D building models, key segments and vertices of the roofs should be acquired from the point clouds. Considering the structure of building models, those segments and vertices can be categorized into two types, i.e. roof intersection segments and vertices, and building boundary segments and vertices. These two types should be processed respectively.

4.1. Roof intersection segments and vertices

To find roof intersection segments, the roof intersection lines are first determined based on the plane parameters of the segmented roofs and then terminals of the roof intersection segments are estimated based on points on the intersection lines. However, due to the disadvantage of airborne LiDAR systems in measuring linear objects, those segments are usually shorter than the true ones. Therefore, the roof intersection vertices are difficult to identify. In order to correctly find the roof intersection vertices, the undirected graph model of the roofs is utilized.

In the graph, each roof denotes a node and two roofs are connected to each other if there exists a segment between them. For example, the building in Figure 2(a) contains four planar roofs and one roof intersection point. Based on the roof intersection segments in Figure 2(a), the corresponding graph is constructed as shown in Figure 2(b). It can be seen that the nodes of the three roofs which determine the roof intersection point form a circle. Therefore, after the graph is constructed, minimal closed circles in the graph are searched and a roof intersection point can be determined by one closed circle. A minimal closed circle is composed of at least three nodes (planes) and therefore a unique point could be identified by intersecting those planes. The graph is constructed based on the topological information and thus the estimated position of the roof intersection point is correct.

In addition to finding the roof intersection points, the undirected graph can also be used to separate single buildings in the building modeling process. When obtaining regular building boundaries, it is preferred that one single building whose roofs are connected is processed rather than several buildings. However, when automatically separating buildings, the connective component analysis is usually utilized and neighboring buildings (usually more than one single building) are likely to be clustered in a group. By searching the connected component of the undirected graph reflecting the roof topological relationship, single buildings can be separated, which will facilitate the building boundary regularization process.

By using the undirected graph, some special roof structures (for example dormers) can also be identified. In most cases, a dormer has only one roof and thus it is not in a loop in the undirected graph. Moreover, the dormer usually has a smaller size than the

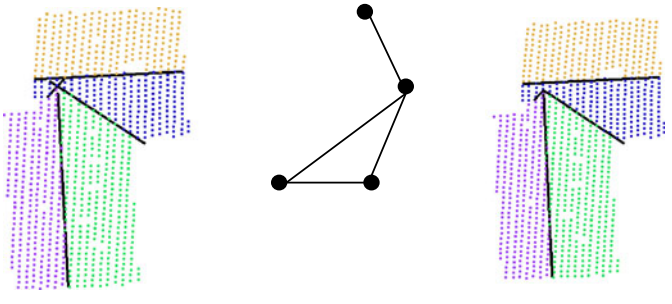

Figure 2. Identification of roof intersection point from the undirected graph: (a) building points and roof intersection segments, (b) the undirected graph (each node denotes a planar roof), and (c) roof intersection point.

roof and if projected to *XY* plane (horizontal plane) its centroid is within the roof. Thus dormers can be identified and reconstructed by using the undirected graph.

4.2. Building boundary segments and vertices

To obtain reasonable and usable models, regular building boundary segments should be obtained from the point clouds. Some methods adjusted the segments according to the domain directions of the buildings. However, these methods do not apply to complex building models, for example, buildings composed of several simple building models. In addition, as assumptions and prior knowledge are used, these methods usually require more parameters. These two problems should be taken into account in building boundary regularization.

In this paper, the building points are first rasterized by the cell size $c = \sqrt{1/p}$ (p refers to the average point density of the point clouds). This cell size can maintain details of the point clouds as well as the information of edges and is widely adopted when rasterizing point clouds. Based on the rasterized data, building boundary points are extracted by a 2D alpha shape algorithm which proves to be efficient for both convex and concave building shapes. The alpha value of the alpha shape algorithm is set as twice the cell size. Then, the RANSAC algorithm is performed to find long segments and the corresponding parameters, for example the distance threshold of a point to the line, can also be set according to the cell size.

Once long segments are obtained, the segments are then adjusted by aligning these segments as parallel or orthogonal to successive segments as possible. To avoid a priori knowledge as much as possible, the parallel mergence and orthogonal adjustments are used in this paper. In the parallel mergence process, if the angle of two successive segments is smaller than a certain threshold (15° in this paper), these two segments are combined into one. In the orthogonal adjustment, the segment connecting two neighboring parallel or orthogonal segments obtained by the RANSAC method may be adjusted according to its length.

After regularized boundaries are obtained, by combining the roof intersection segments and building boundaries, the 3D building roof models are derived. Finally, by extending the building boundaries to the ground surface, 3D polyhedral building models are acquired.

5. Experiments

5.1. Dataset

In this paper, the Vaihingen dataset provided by the German Society for Photogrammetry, Remote Sensing and Geoinformation (DGPF; Cramer 2010) is employed to provide both quantitative and qualitative evaluation of our method. The DGPF dataset is acquired on 21 August 2008 by Leica Geosystems using a Leica ALS50 system with 45° field of view and a mean flying height above ground of 500 m. The mean point density in one strip is four points per square meter. The data of Area 3 which is a purely residential area with small detached houses are segmented by our method and furthermore the 3D building models are also reconstructed to provide quantitative evaluation of the segmentation method and the model generation method.

5.2. Experiments

As our segmentation approach aims to extract roofs from building points, the progress Triangulated Irregular Network (TIN) filter (Axelsson 2000) is firstly carried out to separate ground points and then building points are obtained by a region growing algorithm. After the building points are extracted, the MoG segmentation method, including the EM classification, nonplanar objects removal, and coplanar patches mergence, is performed to separate planar roofs.

The most important parameter of our method is the number of Gaussian components when performing the EM algorithm. For most of the buildings which possess a sufficient number of points in the dataset, the minimum number of Gaussian components $K_{\min}$ is set as four and the maximum $K_{\max}$ is nine since the maximum number of roofs of buildings is five. For the buildings consisting of only one roof, $K_{\min}$ is two while $K_{\max}$ is four. The angle threshold of coplanar planes is 10° and the planarity of a planar roof should be smaller than 0.001.

Once the building roofs are segmented, 3D building models are reconstructed by combining regularized building outlines and roof intersections.

6. Results and discussion

Both quantitative and qualitative evaluation methods are employed to validate the performance of the segmentation method and the model generation on the real dataset. First, based on the evaluation results of the International Society for Photogrammetry and Remote Sensing (ISPRS) Working Group III/4, the correctness of the segmentation results is evaluated. In addition, the plane fitting quality of roofs, i.e. the mean and standard deviation of distance of the points to the corresponding roofs, indicates whether the segmentation results obtain planar objects whose mean and standard deviation values are small and within tolerance. Second, the number of roof intersections is also counted to assess the performance of the segmentation methods for the neighboring roof points. The segmentation results of both our method and the popular RANSAC method are evaluated and compared. Finally, the accuracy of the final building models is discussed.

In terms of the segmentation correctness, as demonstrated in Table 1, the correctness of the processed buildings is 100%, which demonstrates that all detected roofs are correctly separated. Moreover, by comparing the yellow pixels in Figure 3(b) with Figure 3(a), it can be seen that for the detected buildings, our segmentation method obtains correct roof segmentation results and no roofs are misdetected or neglected. This can also be concluded from the fact as shown in Figure 3(b) in which the red blocks represent falsely detected roofs that only exist in the building boundaries. It should be noted that for the blue blocks referring to misdetected roofs in Figure 3(b), the corresponding area in Figure 3(a) does not contain sufficient points because some points

Table 1. Vaihingen results: 3D building reconstruction in Area 3.

Compl. roof [%]	Corr. roof [%]	Compl. roof 10 [%]	Corr. roof 10 [%]
73.2	100	83.1	100

Note: This table is shown on the I ISPRS Working Group III/4 website (http://www2.isprs.org/commissions/comm3/wg4/results/a3_recon.html). Compl. roof [%] shows the completeness of detected roof planes compared to the reference data while Corr. roof [%] displays the correctness of detected roof planes. Compl. roof 10 [%] and Corr. roof 10 [%] exhibit results of large roof planes whose area is larger than 10 m^2.

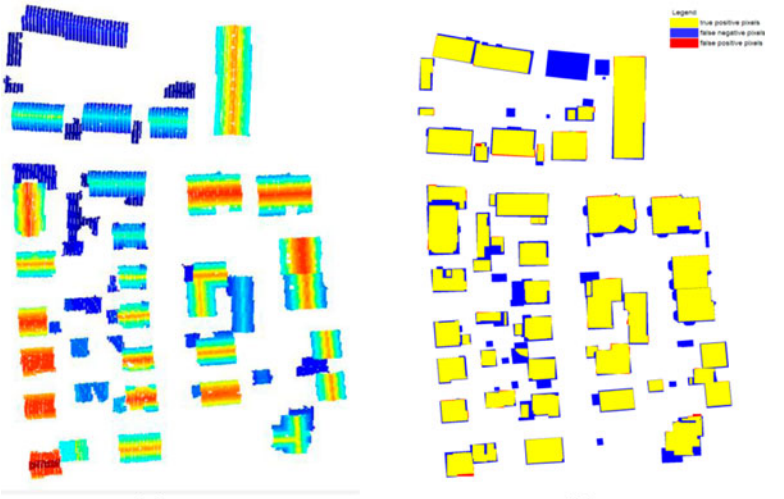

Figure 3. Evaluation of reconstructed models: (a) detected building points and (b) evaluation of the reconstructed models on a per-pixel level.

are missing during data collection and some points are classified as nonbuilding points when removing ground points and detecting building points.

To fully inspect the segmentation results, the plane fitting quality is also computed. As shown in Figure 4, the plane fitting quality of the segmentation results is high, as the average of mean distance of the points to the corresponding roofs is about 0.02 m and the values of the corresponding standard deviation are nearly zero. High plane fitting quality indicates that the MoG segmentation method is able to separate nearly planar objects. However, several buildings display high mean values larger than 0.05 m while the maximum is 0.147 m, and high values of the standard deviation which are larger than 0.005 m and the maximum is 0.019 m. These buildings are small and possess fewer points and therefore some points with larger deviations to the plane can lead to higher overall mean and standard deviation values.

Effective segmentation methods should obtain correct numbers of roof intersections which ensure the correctness and accuracy of the final models. To further validate the

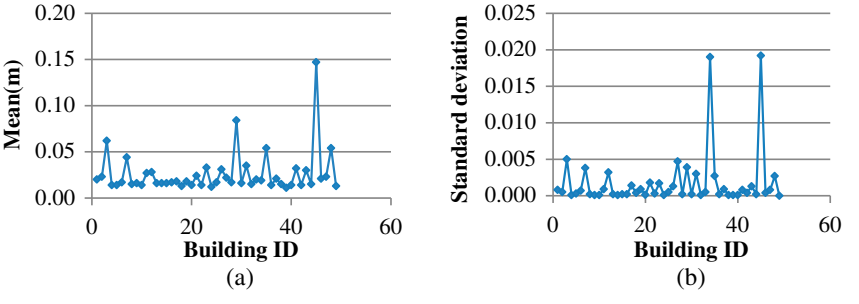

Figure 4. Plane fitting quality: (a) the mean distance (in meters) of the points to the corresponding roofs and (b) the standard deviation of the distance of points to the corresponding roofs.

proposed segmentation method as to whether the segmentation results are able to obtain the key segments and thus maintain accurate topological relationships, roof intersection lines of buildings should also be inspected. If the segmentation method successfully extracts planar roofs, intersection lines of roofs containing sufficient points will be identified by intersecting the roofs. In our experiment, the distance threshold of a point belonging to an intersection line is set as 0.4 m and lines containing less than two points from either of the two planes are ignored.

Roof intersections of the 27 gable buildings in the dataset are computed and the number of lines is also estimated and compared to the true number of roof intersections. Experimental results in Figure 5 of the roof intersections from the segmentation results demonstrate that the proposed method nearly obtains the correct number of roof intersections. The only discrepancy occurs as building 11 contains a small dormer and the roof intersection segment does not contain sufficient points and thus is not detected. The MoG method utilizes the Mahalanobis distance to separate neighboring roof points. Due to the data covariance matrix, minor deviations in elevation could lead to large possibilities of points belonging to a cluster. Therefore, the neighboring roofs are successfully separated and the roof intersection segments are correctly identified.

On the contrary, the RANSAC algorithm acquires fewer intersections as shown in Figure 5. The RANSAC algorithm usually fails to separate roofs when neighboring roofs possess similar slope as the algorithm assigns a point to a candidate shape according to the deviation of the point to the shape and the normal vector difference. Thus in the experiments, some dormers are not correctly separated because they have a small angle with the roof. For example, for the building in Figure 6(a), RANSAC only detects two roofs as the dormer and the roofs are segmented as one class. Therefore, the plane equation of the new cluster is quite different from the real roof, and no intersection is detected as shown in Figure 6(a). Also, RANSAC usually falsely classifies the neighboring roof points, and the roof intersection location is not so accurate. These are the reasons that the RANSAC algorithm only finds one roof intersection instead of three when segmenting the building in Figure 6(b). Even though the two dormers are correctly extracted, the intersections are not identified because some neighboring roof points are assigned to the roofs and thus there are few or no points of the dormers on the corresponding intersections.

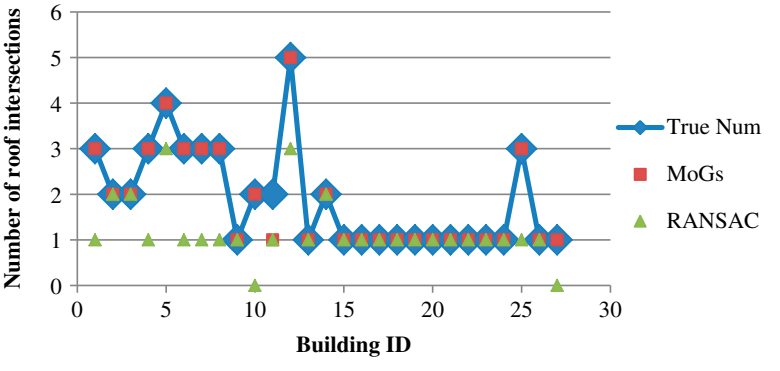

Figure 5. Number of roof intersections.

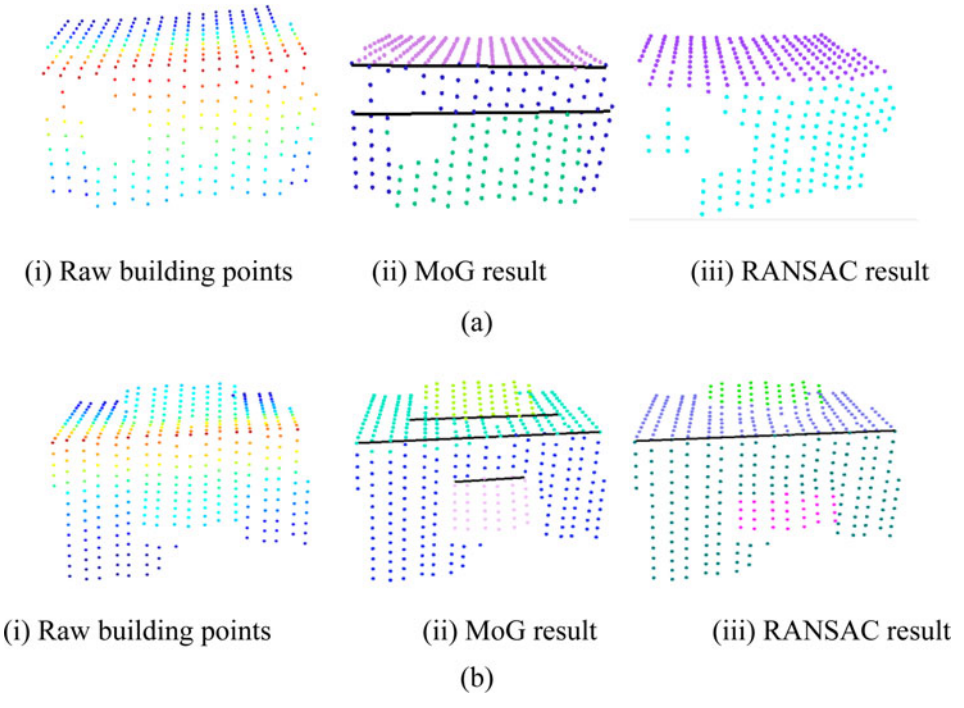

Figure 6. Roof intersection results of two buildings: (a) roof intersections (black lines) of building 10 and (b) roof intersections (black lines) of building 8.

Apart from the evaluation of the segmentation results, quantitative evaluations of the building models are also provided by the ISPRS Working Group III/4 as shown in Table 2. The fact that the planimetric accuracy of the models is high (0.8 m) demonstrates that our boundary regularization method is able to obtain correct boundaries. Although to some extent rasterization of the point clouds can lead to data loss, reconstructed boundaries still have a high accuracy because the adjustment of the boundary segments may compensate this loss and thus the obtained building boundaries have a high accuracy. The vertical accuracy of building models is mainly determined by the roof intersection points. Our models have a high vertical accuracy (0.1 m) which proves that by using the graph the roof intersection points are correctly identified.

7. Conclusions and future work

To obtain accurate 3D building models from airborne LiDAR data, this paper presents a novel segmentation method of building roofs and a generic model generation method. By using the MoG model to depict building roof points, this segmentation method successfully separates roof points into several planar segments and identifies intersection lines of roofs. To obtain regular building models, rasterized data are utilized to facilitate the process and maintain its applicability. In addition, a graph of the roof topology is introduced to identify roof intersection points. Finally, 3D polyhedral building models are obtained.

Table 2. Accuracy of final building models.

Abbrev.	RMS [*m*]	RMSZ [*m*]
CKU	0.8	0.6
FIE	1.1	0.3
ITC1	0.8	0.1
ITC2	1.0	0.2
ITCX	0.7	0.1
ITCX_G1	0.7	0.1
ITCX_G2	0.7	0.1
TUD	0.7	0.1
VSK	0.8	0.1
YOR	0.6	0.2
CAS_YX	***0.8***	***0.1***
MON_13	0.9	0.3
KNTU	0.9	0.4
BNU	0.6	0.1

Note: This table and the corresponding details can be referred on http://www2.isprs.org/commissions/comm3/wg4/results/a3_recon.html. Bold faces refer the evaluation results of the models generated by our methods. Abbrev. denotes the short name of the results provider. Root mean square (RMS) [*m*] denotes planimetric geometric accuracy in *XY* plane while RMSZ [*m*] denotes geometric accuracy of Z component.

The experimental results of the study area show that the proposed segmentation is able to extract planar roofs and obtain correct roof intersection segments. Quantitative evaluation of the building models demonstrates that the model generation method has a high accuracy. In future, we will focus on applying the segmentation and model generation method to more data.

Acknowledgments

We are grateful to the three reviewers for constructive comments and advice on the manuscript. The Vaihingen dataset was provided by the DGPF [Cramer 2010]; http://www.ifp.uni-stuttgart.de/dgpf/DKEP-Allg.html (in German).

Funding

This work was supported by the National Key Scientific Instrument and Equipment Development Projects of China [grant number 2013YQ120343]; the National Natural Science Foundation of China [grant numbers 41171265 and 41101436]; and the 100 Talents Program of the Chinese Academy of Sciences.

References

Alharthy, A., and J. Bethel. 2002. "Heuristic Filtering and 3D Feature Extraction from LiDAR Data." *International Archives of Photogrammetry Remote Sensing and Spatial Information Sciences* 34 (3/A): 29–34.

Alharthy, A., and J. Bethel. 2004. "Detailed Building Reconstruction from Airborne Laser Data Using a Moving Surface Method." *The International Archives of the Photogrammetry, Remote Sensing and Spatial Information Sciences* 34B: 213–218.

Alpaydin, E. 2004. *Introduction to Machine Learning*. Cambridge, MA: The MIT Press.

Ameri, B., and D. Fritsch. 2000. *Automatic 3D Building Reconstruction Using Plane-Roof Structures*. Washington, DC: ASPRS Annual Conference, 22–26.

Axelsson, P. 2000. "Dem Generation from Laser Scanner Data Using Adaptive Tin Models." *International Archives of Photogrammetry and Remote Sensing* 33 (B4/1; PART 4): 111–118.

Bishop, C. M. 2006. *Pattern Recognition and Machine Learning*. New York: Springer.

Brenner, C. 2000. "Towards Fully Automatic Generation of City Models." *International Archives of Photogrammetry and Remote Sensing* 33 (B3/1; PART 3): 84–92.

Charaniya, A. P. 2004. *3D Urban Reconstruction from Aerial LiDAR Data*. Santa Cruz: University of California.

Chen, D., L. Zhang, J. Li, and R. Liu. 2012. "Urban Building Roof Segmentation from Airborne LiDAR Point Clouds." *International Journal of Remote Sensing* 33 (20): 6497–6515. doi:10.1080/01431161.2012.690083.

Cramer, M. 2010. "The DGPF Test on Digital Aerial Camera Evaluation – Overview and Test Design." *Photogrammetrie – Fernerkundung – Geoinformation* 2010 (2): 73–82. doi:10.1127/1432-8364/2010/0041.

Dempster, A. P., N. M. Laird, and D. B. Rubin. 1977. "Maximum Likelihood from Incomplete Data via the EM Algorithm." *Journal of the Royal Statistical Society. Series B (Methodological)* 39: 1–38.

Dorninger, P., and N. Pfeifer. 2008. "A Comprehensive Automated 3D Approach for Building Extraction, Reconstruction, and Regularization from Airborne Laser Scanning Point Clouds." *Sensors* 8 (11): 7323–7343. doi:10.3390/s8117323.

Fischler, M. A., and R. C. Bolles. 1981. "Random Sample Consensus: A Paradigm for Model Fitting with Applications to Image Analysis and Automated Cartography." *Communications of the ACM* 24 (6): 381–395. doi:10.1145/358669.358692.

Gamba, P., and B. Houshmand. 2000. "Digital Surface Models and Building Extraction: A Comparison of IFSAR and LIDAR Data." *IEEE Transactions on Geoscience and Remote Sensing* 38 (4): 1959–1968. doi:10.1109/36.851777.

Grünwald, P. D. 2007. *The Minimum Description Length Principle*. Cambridge, MA: The MIT Press.

Kim, K., and J. Shan. 2011. "Building Roof Modeling from Airborne Laser Scanning Data Based on Level Set Approach." *ISPRS Journal of Photogrammetry and Remote Sensing* 66 (4): 484–497. doi:10.1016/j.isprsjprs.2011.02.007.

Lloyd, S. 1982. "Least Squares Quantization in PCM." *IEEE Transactions on Information Theory* 28 (2): 129–137. doi:10.1109/TIT.1982.1056489.

Lodha, S. K., D. M. Fitzpatrick, and D. P. Helmbold. 2007. "Aerial LiDAR Data Classification Using Expectation-Maximization." *In Proceedings of the SPIE Conference on Vision Geometry XIV* 6499, L1–L11, January 2007.

Maas, H.-G., and G. Vosselman. 1999. "Two Algorithms for Extracting Building Models from Raw Laser Altimetry Data." *ISPRS Journal of Photogrammetry and Remote Sensing* 54 (23): 153–163. doi:10.1016/S0924-2716(99)00004-0.

Oda, K., T. Takano, T. Doihara, and R. Shibaski. 2004. "Automatic Building Extraction and 3-D City Modeling from LiDAR Data Based on Hough Transform." *International Archives of Photogrammetry and Remote Sensing* XXXV (B3): 277–281.

Overby, J., L. Bodum, E. Kjems, and P. Iisoe. 2004. "Automatic 3d Building Reconstruction from Airborne Laser Scanning and Cadastral Data Using Hough Transformed." *International Archives of Photogrammetry and Remote Sensing* XXXV (B3): 1–6.

Rabbani, T., and F. Van Den Heuvel. 2005. "Efficient Hough Transform for Automatic Detection of Cylinders in Point Clouds." *ISPRS WG III/3, III/4* 3: 60–65.

Rissanen, J. 1983. "A Universal Prior for Integers and Estimation by Minimum Description Length." *The Annals of Statistics* 11 (2): 416–431. doi:10.1214/aos/1176346150.

Roth, G., and M. D. Levine. 1993. "Extracting Geometric Primitives." *CVGIP: Image Understanding* 58 (1): 1–22. doi:10.1006/ciun.1993.1028.

Sampath, A., and J. Shan. 2004. "Urban Modeling Based on Segmentation and Regularization of Airborne LiDAR Point Clouds." In *XXth ISPRS Congress*, *Istanbul, Turkey*, CD-ROM.

Sampath, A., and J. Shan. 2010. "Segmentation and Reconstruction of Polyhedral Building Roofs from Aerial LiDAR Point Clouds." *IEEE Transactions on Geoscience and Remote Sensing* 48 (3): 1554–1567. doi:10.1109/TGRS.2009.2030180.

Schnabel, R., R. Wahl, and R. Klein. 2007. "Efficient RANSAC for Point-Cloud Shape Detection." *Computer Graphics Forum* 26 (2): 214–226. doi:10.1111/j.1467-8659.2007.01016.x.

Sester, M., and H. Neidhart. 2008. "Reconstruction of Building Ground Plans from Laser Scanner Data." *11th AGILE International Conference on Geographic Information Science*, University of Girona, Spain, 2008.

Tarsha-Kurdi, F., T. Landes, and P. Grussenmeyer. 2008. Extended RANSAC Algorithm for Automatic Detection of Building Roof Planes from LiDAR Data." *Photogrammetric Journal of Finland* 21 (1): 97–109.

Verma, V., R. Kumar, and S. Hsu. 2006. "3D Building Detection and Modeling from Aerial LiDAR Data." *Proceedings of the 2006 IEEE Computer Society Conference on Computer Vision and Pattern Recognition* 2: 2213–2220.

Vosselman, G., and S. Dijkman. 2001. "3D Building Model Reconstruction from Point Clouds and Ground Plans." *International Archives of Photogrammetry Remote Sensing and Spatial Information Sciences* 34 (3/W4): 37–44.

Wang, R. 2013. "3D Building Modeling Using Images and LiDAR: A Review." *International Journal of Image and Data Fusion* 4 (4): 273–292. doi:10.1080/19479832.2013.811124.

Zhang, K., J. Yan, and S.-C. Chen. 2006. "Automatic Construction of Building Footprints from Airborne LiDAR Data." *IEEE Transactions on Geoscience and Remote Sensing* 44 (9): 2523–2533. doi:10.1109/TGRS.2006.874137.

Zhou, Q. Y., and U. Neumann. 2008. "Fast and Extensible Building Modeling from Airborne LiDAR Data." *ACM SIGSPATIAL International Conference on Advances in Geographic Information Systems*, 1–8. New York, NY: Penn Plaza.